Liquid Crystals
Publication details, including instructions for authors and subscription information:
http://www.informaworld.com/smpp/title~content=t713926090

Conformational behaviour of laterally dialkoxy branched mesogens. Part two

H. Allouchi; M. Cotrait; E. Lafontaine; P. Berdague; J. -P. Bayle

Online publication date: 06 August 2010

To cite this Article Allouchi, H. , Cotrait, M. , Lafontaine, E. , Berdague, P. and Bayle, J. -P.(2001) 'Conformational behaviour of laterally dialkoxy branched mesogens. Part two', Liquid Crystals, 28: 6, 851 — 860
To link to this Article: DOI: 10.1080/02678290110046284
URL: http://dx.doi.org/10.1080/02678290110046284

LIQUID CRYSTALS, 2001, VOL. 28, NO. 6, 851–860

Conformational behaviour of laterally dialkoxy branched mesogens. Part two†

H. ALLOUCHI

Laboratoire de Chimie Physique, PIMIR E. A. 2098,
Faculté des Sciences Pharmaceutiques, 31 avenue Monge, 37200 Tours, France

M. COTRAIT

Laboratoire de Chimie Organique et Organométallique, UMR 5802 CNRS. 351,
Cours de la Libération, Université Bordeaux I, 33405 TALENCE Cedex, France.

E. LAFONTAINE

DGA/CREA, 16 bis Avenue Prieur de la Côte d'Or, 91414 Arcueil Cedex, France

P. BERDAGUÉ and J.-P. BAYLE*

Laboratoire de Chimie Structurale Organique, URA CNRS 1384,
Université Paris XI, Bât. 410, 91405 Orsay Cedex, France

(*Received 9 October 2000; accepted 11 January 2001*)

The crystal structures of 2,3-*n*-diheptyloxy-4-(4-chlorobenzoyloxy)-4′-(4-methylbenzoyloxy)-azobenzene ($C_{41}H_{47}N_2O_2Cl$, labelled 7DIAB) and of 2,3-*n*-dioctyloxy-4-(4-chlorobenzoyloxy)-4′-(4-methylbenzoyloxy)azobenzene ($C_{43}H_{51}N_2O_2Cl$, labelled 8DIAB) have been solved. 7DIAB crystallizes in the $P2_1/a$ space group with $Z = 8$, $a = 18.577(2)$, $b = 32.727(2)$, $c = 13.654(2)$ Å and $\beta = 106.01(1)°$; 8DIAB crystallizes in the $P2_1/c$ space group with $Z = 8$, $a = 13.689(1)$, $b = 33.448(3)$, $c = 18.922(5)$ Å and $\beta = 104.94(4)°$. There are two independent molecules in the asymmetric unit for both compounds. The final reliability factors were $R = 0.083$ and 0.106, respectively for 7DIAB and 8DIAB. These molecules present the same polyaromatic core, but differ in the length of the two lateral alkoxy chains containing, respectively, seven and eight carbons. The polyaromatic cores are quite linear with a length close to 24.7 Å. One of the long alkoxy lateral chains is folded back to the core, while the other one, more or less extended, makes an angle close to 70° with the core, for both structures. The molecular conformations of both 7DIAB and 8DIAB are quite different from those of molecules with shorter lateral alkoxy chains (containing five and six carbons) for which both chains are folded back to the polyaromatic core. This shows the great flexibility of the alkoxy lateral chains. ^{13}C NMR probes the existence of different conformations in the solid phase and indicates that the mean chain conformation in the nematic phase is nearly independent of the chain lengths.

1. Introduction

Nematogens based on a molecule bearing lateral flexible substituents cannot be compared in a simple way to rod-like molecules [1–4]. Even if the nematophase exists due to the molecular anisotropy, this anisotropy can be enforced by the nematic field itself. This means that in the nematic phase the lateral chains are folded back along the core to preserve both the anisotropy and the best packing which are necessary conditions for the thermodynamic existence of the mesophase. In the solid phase, X-ray structures usually give a relevant picture of the molecular arrangement which exists in the liquid crystal phase. Thus, a study of the chain conformations in the solid phase of the lateral substituents is of prime importance to understand the origin of the liquid crystal properties.

In the preceding paper, we presented the structures of two compounds containing four rings in the main core and two short lateral chains [5], $R = C_5H_{11}$ (5DIAB) and $R = C_6H_{13}$ (6DIAB) (figure 1).

* Author for correspondence; e-mail: jpbayle@icmo.u-psud.fr

† For part I see ref. [5].

Liquid Crystals ISSN 0267-8292 print/ISSN 1366-5855 online © 2001 Taylor & Francis Ltd
http://www.tandf.co.uk/journals
DOI: 10.1080/02678290110046284

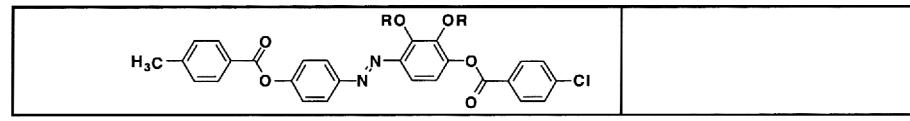

Figure 1. Generic formula of the compounds studied.

It was found that in both structures the central core is extended and quite rigid. The two lateral chains are folded back along the core as expected to give the liquid crystal phase and exhibit slightly different conformations. This molecular arrangement is characteristic of a nematogenic system. To assume such folding, the first fragments within the chains are in *gauche* conformations. To avoid steric interactions, the first two CH_2 groups lie above and below the mean plane defined by the substituted aromatic ring. We have shown that it is also possible to follow the chain conformations in the different phases by the ^{13}C NMR of the $-OCH_2-$ carbons [6, 7] for compounds having a single lateral chain. However, the results obtained for 5DIAB and 6DIAB containing two nearby lateral chains show that the $-OCH_2-$ signal is very sensitive both to the conformation of the lateral chain and to the local geometry of the nearby oxygen bearing the second lateral chain [5]. Nevertheless, after the solid–nematic transition, the frequencies of the first two lateral carbons are nearly the same, indicating that the mean conformation in the nematic phase is rather independent of the remote parts of the molecule. On cooling, the lateral chains can be trapped in several conformations giving a complex pattern in the $-OCH_2-$ region [5], indicating that during the solidification process, several different conformations of the $-OCH_2-$ fragment can be obtained.

In this paper, we will investigate the X-ray structures of two compounds belonging to the same series, but having longer alkoxy chains, i.e. $R = C_7H_{15}$ (7DIAB) and $R = C_8H_{17}$ (8DIAB), in which, as we shall see later, the lateral chains behave differently. The conformational behaviour will be followed in the polycrystalline samples by ^{13}C NMR in the solid and nematic phases of the above two compounds and in 12DIAB.

2. Experimental

2.1. *Crystal structure determination and refinement*

Suitable crystals of 7DIAB and 8DIAB were grown from $CHCl_3$ solutions at 293 K. The crystal setting, the cell parameters and the data collection were performed with a CAD-4 Enraf-Nonius diffractometer, equipped with a graphite monochromator for the CuK_α radiation. The crystal data, data collection and refinement characteristics are given in table 1. In both crystal structures, the asymmetric unit contains two independent molecules **1** and **2**. Twenty-five reflections with θ between 24° and 34° for 7DIAB and between 25° and 41° for 8DIAB were used for the crystal setting and the least-squares refinement of cell parameters. The absorption correction was performed using the *y*-scan technique [8].

Both structures were solved by direct methods, using the MITHRIL package [9], which led to the position of all atoms of the core and a few atoms at the beginning of the alkoxy lateral chains. The remaining atoms were located with great difficulty after successive Fourier syntheses. The atomic parameters were refined with the SHELX93 package [10] with anisotropic thermal parameters for the non-hydrogen atoms†, using constraints on the C–C bond lengths of the alkyl chains. The final reliability factors were $R = 0.083$ for 7DIAB and 0.106 for 8DIAB structures.

2.2. *^{13}C NMR spectra*

High resolution ^{13}C NMR spectra were obtained with a Bruker MSL 200 spectrometer using a double-tuned coil MAS probe for ^{13}C and ^{1}H NMR. The crystalline samples were filled into fused zirconia rotors fitted with boron nitride caps and spun at 6 kHz at the magic angle (54.7°). ^{13}C chemical shifts were referenced to the glycine carbonyl signal (assigned at 176.03 ppm) used as an external reference. For each spectrum, 512 scans were accumulated using a cross-polarization pulse (with a ^{1}H 90° pulse of 4.1 ms), high power decoupling during acquisition, 0.03 s acquisition, 3 s recycle delay and 1.2 ms mixing time. Variable temperature CP/MAS NMR experiments were performed in the 30–150°C range using a Eurotherm thermal controller calibrated with the 1,4-diazabicyclo-(2,2,2)-octane (DABCO) crystal–crystal transition [11].

3. Results and discussion

3.1. *Structure analysis*

The fractional coordinates and the equivalent thermal motion factors B_{eq} are given in table 2 for 7DIAB and in table 3 for 8DIAB. The B_{eq} atomic factors for the polyaromatic cores in both structures are quite low; those of the lateral alkoxy chains increase progressively from the beginning to their ends to an extent such that the chains can be considered quite disordered.

The labelling of non-hydrogen atoms is presented in figure 2 along with a stick-and-ball representation of the

† The hydrogen atoms were placed in their theoretical positions and allowed to ride on the carbon atoms to which they are attached, according to the SHELX93 program [10].

Table 1. Crystal data, data collection and refinement characteristics.

Data collection	7DIAB	8DIAB
Chemical formula	$C_{41}H_{47}N_2O_6Cl$	$C_{43}H_{51}N_2O_6Cl$
Molecular mass ($g\,mol^{-1}$)	699.3	727.3
Crystal system	monoclinic	monoclinic
Space group	$P2_1/a$	$P2_1/c$
Z	8	8
a (Å)	18.577(2)	13.689(11)
b (Å)	32.727(2)	33.448(3)
c (Å)	13.654(2)	18.922(5)
β (°)	106.01(1)	104.94(4)
Volume of cell (Å^3)	7979	8371
Density ($g\,cm^{-3}$)	1.164	1.154
Absorption μ(mm^{-1})	1.22	1.18
h_{min}; h_{max}	−18; 18	0; 16
k_{min}; k_{max}	0; 32	0; 39
l_{min}; l_{max}	0; 13	−22; 22
θ_{max} (°)	50	65
Measured reflections	8201	13615
Observed reflections	4157	4183
Criteria	$I > 3\sigma(I)$	$I > 3\sigma(I)$
R_{int} (%)	1.15	1.12
Refinement	on F^2	on F^2
Hydrogen refinement	no	no
Weight	$1/\sigma(F_o^2)^2 + (0.146P)^2 + 16.95P$ $P = [\mathrm{Max}(F_o^2, 0) + 2F_c^2]/3$	$1/\sigma(F_o^2)^2 + (0.22P)^2 + 17.70P$ $P = [\mathrm{Max}(F_o^2, 0) + 2F_c^2]/3$
R	0.083	0.106
S	1.141	1.112
Temperature (K)	293	293

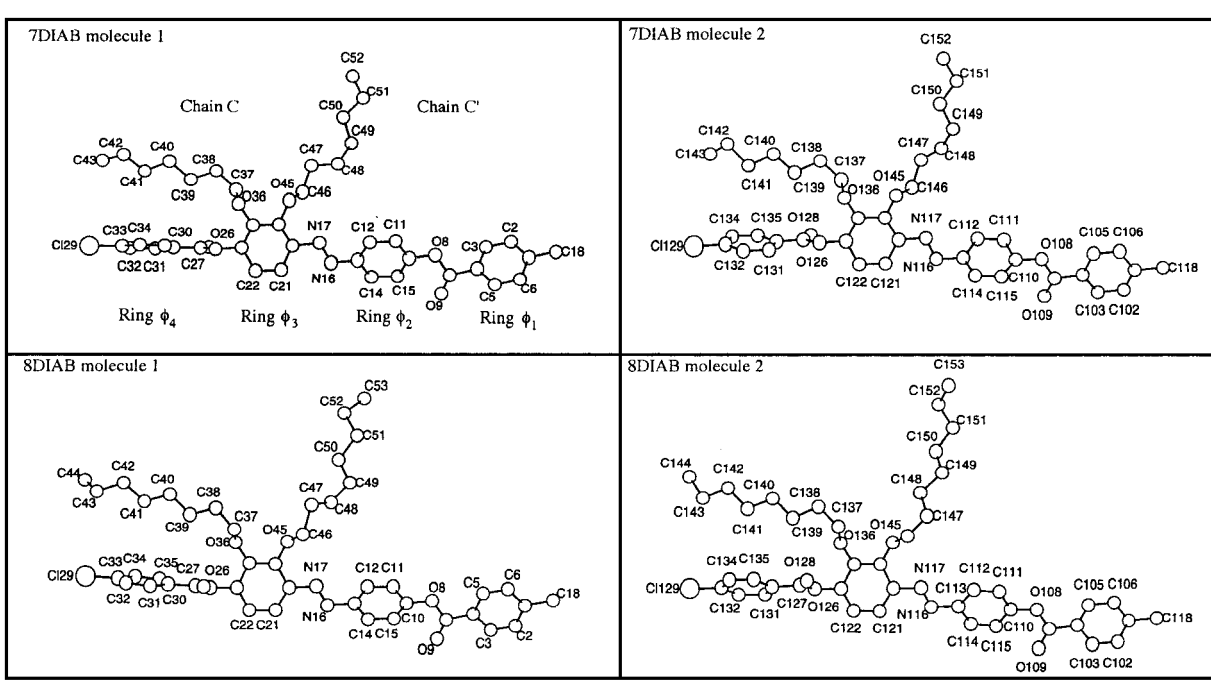

Figure 2. Stick-and-ball representation and atomic labelling for both independent molecules **1** and **2** in the 7DIAB and 8DIAB structures.

Table 2. Fractional atomic coordinates and B_{eq} factors for 7DIAB.

Atom	*x/a*	*y/b*	*z/c*	B_{eq}/Å^2
C1	0.8065(5)	0.8098(3)	−0.0694(8)	5.7(5)
C2	0.8124(5)	0.7788(3)	−0.1360(8)	5.9(5)
C3	0.8267(5)	0.7395(3)	−0.1028(8)	5.8(5)
C4	0.8362(5)	0.7291(3)	−0.0049(6)	4.6(4)
C5	0.8322(5)	0.7595(3)	0.0635(7)	5.5(5)
C6	0.8168(5)	0.7988(3)	0.0301(8)	6.2(5)
C7	0.8531(5)	0.6866(3)	0.0327(7)	5.2(5)
O8	0.8468(4)	0.6602(2)	−0.0448(5)	6.1(3)
O9	0.8701(4)	0.6763(2)	0.1209(5)	7.3(4)
C10	0.8607(5)	0.6191(3)	−0.0219(7)	5.5(5)
C11	0.8021(6)	0.5920(3)	−0.0590(9)	7.3(6)
C12	0.8160(6)	0.5513(3)	−0.0458(9)	7.7(6)
C13	0.8848(5)	0.5367(3)	0.0047(7)	5.5(5)
C14	0.9423(5)	0.5637(3)	0.0381(7)	5.6(5)
C15	0.9313(5)	0.6052(3)	0.0247(7)	5.8(5)
N16	0.9022(4)	0.4945(2)	0.0228(6)	5.7(4)
N17	0.8538(4)	0.4713(2)	−0.0338(6)	6.3(4)
C18	0.7911(7)	0.8529(4)	−0.1026(10)	8.9(7)
C20	0.8679(5)	0.4283(3)	−0.0114(8)	5.7(5)
C21	0.9075(6)	0.4145(3)	0.0817(8)	6.0(5)
C22	0.9154(6)	0.3732(3)	0.0983(8)	6.4(5)
C23	0.8820(5)	0.3464(3)	0.0214(8)	5.4(5)
C24	0.8427(5)	0.3597(3)	−0.0730(8)	5.6(5)
C25	0.8352(6)	0.4012(3)	−0.0878(7)	5.8(5)
O26	0.8857(4)	0.3045(2)	0.0426(5)	6.5(3)
C27	0.9376(5)	0.2821(3)	0.0152(7)	5.4(5)
O28	0.9836(4)	0.2977(2)	−0.0203(6)	7.0(4)
Cl29	0.9189(2)	0.1040(1)	0.0845(4)	13.5(3)
C30	0.9314(5)	0.2386(3)	0.0334(7)	4.9(4)
C31	0.9858(5)	0.2122(3)	0.0175(8)	6.2(5)
C32	0.9826(6)	0.1710(3)	0.0327(10)	7.9(6)
C33	0.9224(6)	0.1562(3)	0.0627(9)	7.8(6)
C34	0.8681(6)	0.1816(3)	0.0793(9)	7.2(6)
C35	0.8736(5)	0.2222(3)	0.0640(8)	5.8(5)
O36	0.8095(4)	0.3318(2)	−0.1474(5)	6.4(3)
C37	0.8438(6)	0.3274(3)	−0.2299(8)	7.2(6)
C38	0.8091(7)	0.2914(4)	−0.2906(8)	8.0(7)
C39	0.8133(6)	0.2515(4)	−0.2327(9)	7.9(6)
C40	0.7863(7)	0.2140(4)	−0.2980(10)	10.0(8)
C41	0.7902(9)	0.1758(4)	−0.2345(12)	12.0(9)
C42	0.7576(13)	0.1383(8)	−0.2865(17)	23.1(19)
C43	0.7750(27)	0.1068(15)	−0.2542(43)	57.1(54)
O45	0.7874(6)	0.4132(2)	−0.1822(6)	11.3(6)
C46	0.8073(9)	0.4348(7)	−0.2391(17)	20.0(15)
C47	0.7373(15)	0.4426(7)	−0.3354(14)	21.6(17)
C48	0.7071(30)	0.4834(13)	−0.3425(54)	57.5(67)
C49	0.6948(29)	0.5018(15)	−0.4488(54)	64.0(70)
C50	0.6342(22)	0.4826(9)	−0.5259(41)	40.9(42)
C51	0.5815(35)	0.5101(22)	−0.6032(69)	71.8(98)
C52	0.5182(43)	0.4874(29)	−0.6732(36)	89.7(93)
C101	−0.1513(6)	0.8227(3)	0.6102(8)	6.5(5)
C106	−0.1992(6)	0.7913(3)	0.5672(8)	6.7(6)
C105	−0.1784(5)	0.7506(3)	0.5859(7)	5.9(5)
C104	−0.1095(5)	0.7414(3)	0.6507(7)	5.4(5)
C103	−0.0630(5)	0.7728(3)	0.6935(7)	6.1(5)
C102	−0.0844(6)	0.8131(3)	0.6729(9)	7.0(6)
C107	−0.0837(5)	0.6987(3)	0.6748(7)	5.6(5)
O108	−0.1344(4)	0.6709(2)	0.6257(5)	6.3(3)
O109	−0.0252(4)	0.6897(2)	0.7329(6)	7.6(4)

Table 2. (*continued*).

Atom	*x/a*	*y/b*	*z/c*	B_{eq}/Å^2
C110	−0.1145(5)	0.6294(3)	0.6371(7)	5.6(5)
C111	−0.1070(6)	0.6093(3)	0.5528(7)	6.0(5)
C112	−0.0909(6)	0.5678(3)	0.5585(7)	6.1(5)
C113	−0.0811(5)	0.5475(3)	0.6500(7)	5.4(5)
C114	−0.0892(7)	0.5684(3)	0.7338(8)	6.9(6)
C115	−0.1054(7)	0.6099(3)	0.7269(8)	7.3(6)
N116	−0.0625(4)	0.5056(2)	0.6663(6)	5.9(4)
N117	−0.0715(4)	0.4854(2)	0.5860(6)	5.9(4)
C118	−0.1751(8)	0.8664(4)	0.5902(10)	9.7(8)
C120	−0.0510(5)	0.4432(3)	0.6036(7)	5.2(5)
C121	0.0032(6)	0.4297(3)	0.6872(7)	6.4(5)
C122	0.0173(6)	0.3885(3)	0.7032(7)	6.5(5)
C123	−0.0226(6)	0.3610(3)	0.6355(7)	5.8(5)
C124	−0.0756(5)	0.3727(3)	0.5477(7)	5.0(5)
C125	−0.0881(5)	0.4148(3)	0.5317(7)	5.2(5)
O126	−0.0138(4)	0.3194(2)	0.6589(5)	6.1(3)
C127	0.0365(5)	0.2975(3)	0.6243(7)	5.8(5)
O128	0.0718(4)	0.3123(2)	0.5727(6)	8.9(4)
Cl129	0.0474(3)	0.1219(1)	0.7402(4)	13.8(3)
C130	0.0383(5)	0.2547(3)	0.6549(7)	5.7(5)
C131	0.0023(6)	0.2402(3)	0.7229(8)	6.9(6)
C132	0.0047(7)	0.1991(3)	0.7480(9)	8.3(7)
C133	0.0442(6)	0.1727(3)	0.7065(9)	7.6(6)
C134	0.0806(7)	0.1863(4)	0.6397(10)	9.2(7)
C135	0.0782(7)	0.2272(3)	0.6150(9)	8.2(7)
O136	−0.1156(3)	0.3443(2)	0.4839(5)	5.8(3)
C137	−0.0971(6)	0.3392(3)	0.3899(8)	7.1(6)
C138	−0.1312(6)	0.2998(3)	0.3408(8)	6.8(6)
C139	−0.1059(6)	0.2622(3)	0.4022(8)	7.1(6)
C140	−0.1392(7)	0.2229(3)	0.3511(9)	8.2(7)
C141	−0.1172(10)	0.1858(4)	0.4159(12)	12.6(10)
C142	−0.1551(17)	0.1453(6)	0.3499(20)	22.8(20)
C143	−0.1399(33)	0.1203(17)	0.4050(37)	50.0(58)
O145	−0.1434(4)	0.4251(2)	0.4471(5)	6.6(3)
C146	−0.1235(9)	0.4518(4)	0.3812(10)	12.0(8)
C147	−0.1958(15)	0.4567(5)	0.2941(18)	20.7(18)
C148	−0.2077(25)	0.4872(7)	0.2246(38)	44.4(44)
C149	−0.2883(24)	0.4963(10)	0.1707(51)	48.9(54)
C150	−0.3247(17)	0.4691(5)	0.0912(23)	25.2(21)
C151	−0.3847(12)	0.4878(7)	0.0026(22)	21.8(19)
C152	−0.4222(23)	0.4603(14)	−0.0737(32)	39.7(41)

two independent molecules of 7DIAB and 8DIAB. The ORTEP drawings of the four molecules are not presented because of the very high values of some B_{eq} factors of the terminal parts of all alkoxy chains.

All benzene rings are perfectly planar as well as the C−N=N−C fragment. When going from the terminal methyl group to the terminal chlorine atom along the polyaromatic core, the phenyl rings are successively labelled ϕ_1, ϕ_2, ϕ_3 and ϕ_4 (figure 2). The benzoate groups are roughly planar [12]. The dihedral angles between the mean-planes of contiguous aromatic groups are given in table 4.

The values of the angles show that the polyaromatic cores of both compounds have approximately the same

Table 3. Fractional atomic coordinates and B_{eq} factors for 8DIAB.

Atom	*x/a*	*y/b*	*z/c*	B_{eq}/Å^2
C1	0.5702(10)	0.8022(4)	0.1976(7)	6.5(7)
C2	0.4703(10)	0.7922(4)	0.1854(7)	6.6(7)
C3	0.4391(9)	0.7544(4)	0.1708(7)	6.0(6)
C4	0.5051(8)	0.7234(3)	0.1672(6)	5.2(6)
C5	0.6054(9)	0.7342(4)	0.1797(7)	6.0(6)
C6	0.6369(9)	0.7722(3)	0.1943(7)	5.9(6)
C7	0.4660(9)	0.6831(3)	0.1494(6)	5.4(6)
O8	0.5419(6)	0.6565(2)	0.1577(5)	6.4(4)
O9	0.3794(6)	0.6732(3)	0.1304(5)	7.8(5)
C10	0.5199(8)	0.6171(4)	0.1405(7)	5.8(6)
C11	0.5488(11)	0.5899(4)	0.1978(8)	7.9(8)
C12	0.5350(11)	0.5497(4)	0.1850(7)	7.3(7)
C13	0.4919(8)	0.5362(3)	0.1144(6)	5.4(6)
C14	0.4632(9)	0.5629(4)	0.0582(7)	6.0(6)
C15	0.4785(8)	0.6031(3)	0.0734(7)	5.4(6)
N16	0.4728(7)	0.4948(3)	0.0963(5)	5.8(5)
N17	0.5240(7)	0.4718(3)	0.1417(6)	6.2(5)
C18	0.6068(11)	0.8443(4)	0.2150(8)	8.5(8)
C20	0.5040(9)	0.4308(3)	0.1280(7)	5.7(6)
C21	0.4110(9)	0.4159(4)	0.0880(7)	6.0(6)
C22	0.3949(9)	0.3757(4)	0.0801(7)	6.4(6)
C23	0.4714(10)	0.3501(4)	0.1121(7)	6.3(7)
C24	0.5656(9)	0.3633(4)	0.1523(7)	6.0(6)
C25	0.5783(8)	0.4033(4)	0.1591(7)	5.6(6)
O26	0.4508(6)	0.3089(2)	0.1093(4)	6.5(4)
C27	0.4813(9)	0.2875(3)	0.0590(7)	5.9(6)
O28	0.5166(7)	0.3027(3)	0.0116(5)	7.8(5)
Cl29	0.4184(5)	0.1126(1)	0.0794(3)	14.4(4)
C30	0.4629(8)	0.2443(3)	0.0638(6)	5.2(6)
C31	0.4774(10)	0.2190(4)	0.0088(7)	6.3(7)
C32	0.4653(11)	0.1796(4)	0.0147(8)	7.9(8)
C33	0.4384(11)	0.1635(4)	0.0748(8)	8.1(8)
C34	0.4243(11)	0.1880(4)	0.1287(8)	7.9(8)
C35	0.4359(9)	0.2276(4)	0.1238(7)	6.1(6)
O36	0.6363(6)	0.3357(2)	0.1835(5)	6.9(4)
C37	0.7214(11)	0.3323(4)	0.1526(8)	8.2(8)
C38	0.7823(10)	0.2981(4)	0.1845(8)	8.0(8)
C39	0.7321(11)	0.2590(5)	0.1822(8)	8.6(8)
C40	0.7930(13)	0.2229(5)	0.2082(10)	10.9(11)
C41	0.7383(14)	0.1842(6)	0.2073(11)	11.9(12)
C42	0.7977(27)	0.1464(10)	0.2291(15)	24.8(26)
C43	0.7432(40)	0.1071(9)	0.2129(28)	36.3(42)
C44	0.7456(82)	0.0833(39)	0.2791(72)	86.3(160)
O45	0.6688(7)	0.4153(3)	0.2047(7)	10.1(6)
C46	0.7323(21)	0.4391(8)	0.1837(15)	18.2(19)
C47	0.8349(18)	0.4437(10)	0.2458(20)	23.5(25)
C48	0.8278(84)	0.4708(36)	0.2994(64)	94.9(123)
C49	0.9246(79)	0.4954(23)	0.3207(61)	78.8(114)
C50	1.0103(38)	0.4718(12)	0.3498(26)	30.5(40)
C51	1.1094(54)	0.4944(18)	0.3900(38)	43.3
C52	1.1669(59)	0.4670(21)	0.4525(41)	48.3
C53	1.2136(163)	0.4924(54)	0.5161(117)	129.8
C101	0.8946(10)	0.8138(4)	1.1629(8)	7.2(7)
C102	0.8306(11)	0.8055(4)	1.0962(8)	7.9(8)
C103	0.8088(9)	0.7670(4)	1.0729(7)	6.8(7)
C104	0.8516(8)	0.7352(3)	1.1172(6)	5.4(6)
C105	0.9147(9)	0.7432(4)	1.1828(7)	6.8(7)
C106	0.9367(9)	0.7823(4)	1.2063(7)	7.0(7)
C107	0.8253(9)	0.6942(4)	1.0888(7)	6.3(7)
O108	0.8722(6)	0.6666(2)	1.1371(5)	6.8(4)
O109	0.7670(7)	0.6863(3)	1.0298(5)	7.9(5)
C110	0.8614(9)	0.6260(4)	1.1168(7)	6.2(6)
C111	0.9426(9)	0.6055(4)	1.1096(8)	6.8(7)
C112	0.9363(9)	0.5663(4)	1.0929(8)	6.8(7)
C113	0.8473(8)	0.5458(3)	1.0827(7)	5.7(6)
C114	0.7663(9)	0.5676(4)	1.0904(9)	7.7(8)
C115	0.7698(9)	0.6065(4)	1.1069(8)	7.5(7)
N116	0.8311(7)	0.5048(3)	1.0630(6)	6.5(5)
N117	0.9094(7)	0.4851(3)	1.0701(5)	6.2(5)
C118	0.9195(13)	0.8567(5)	1.1869(10)	10.8(10)
C120	0.8946(8)	0.4443(4)	1.0494(7)	5.8(6)
C121	0.8071(9)	0.4312(4)	0.9972(8)	6.9(7)
C122	0.7927(9)	0.3914(4)	0.9828(8)	7.3(7)
C123	0.8619(9)	0.3646(4)	1.0184(7)	6.4(7)
C124	0.9491(8)	0.3764(4)	1.0703(7)	5.7(6)
C125	0.9657(8)	0.4161(4)	1.0853(6)	5.7(6)
O126	0.8387(6)	0.3234(2)	1.0107(5)	6.9(4)
C127	0.8762(9)	0.3035(4)	0.9634(7)	6.7(7)
O128	0.9289(8)	0.3173(3)	0.9285(6)	9.7(6)
Cl129	0.7595(6)	0.1312(2)	0.9437(4)	16.2(4)
C130	0.8439(9)	0.2597(4)	0.9579(7)	6.1(6)
C131	0.7743(10)	0.2467(4)	0.9924(8)	7.8(8)
C132	0.7500(11)	0.2056(5)	0.9870(10)	9.5(9)
C133	0.7930(12)	0.1806(4)	0.9498(9)	9.1(9)
C134	0.8613(14)	0.1950(5)	0.9167(10)	10.3(10)
C135	0.8861(12)	0.2331(5)	0.9205(9)	9.3(9)
O136	1.0122(5)	0.3472(2)	1.1106(4)	6.2(4)
C137	1.1070(9)	0.3426(4)	1.0920(7)	7.1(7)
C138	1.1545(9)	0.3046(4)	1.1248(7)	7.1(7)
C139	1.0964(11)	0.2681(4)	1.0980(8)	8.0(8)
C140	1.1434(12)	0.2299(4)	1.1290(9)	9.2(9)
C141	1.0834(15)	0.1938(5)	1.1091(12)	12.9(13)
C142	1.1394(21)	0.1559(9)	1.1428(19)	21.3(24)
C143	1.0744(50)	0.1193(18)	1.1279(36)	42.0
C144	1.1236(96)	0.0890(35)	1.1869(73)	78.5
O145	1.0493(6)	0.4273(3)	1.1378(5)	6.8(4)
C146	1.1174(11)	0.4518(5)	1.1115(11)	11.2(10)
C147	1.1926(23)	0.4733(8)	1.1668(17)	19.9(22)
C148	1.2507(27)	0.4533(7)	1.2290(18)	20.8(23)
C149	1.3454(37)	0.4801(12)	1.2689(25)	35.4(43)
C150	1.3931(38)	0.4607(17)	1.3356(34)	40.4(57)
C151	1.4858(38)	0.4789(14)	1.3843(27)	32.5
C152	1.5603(48)	0.4488(17)	1.4225(35)	41.0
C153	1.6632(149)	0.4617(51)	1.4202(111)	111.5

conformation in molecules **1** and **2**. They can be compared to those found in 5DIAB ($\phi_2/\phi_1 = 76.0°$, $\phi_3/\phi_2 = 31.4°$, $\phi_4/\phi_3 = 82.5°$) [5]; the largest difference arises for the dihedral angle between ϕ_3 and ϕ_2. The conformation of chain C′ pointing away from the core seems to perturb the conjugation of the azo link. In all conformers, one of the two alkoxy chains, chain C (figure 2) is folded back to the core and close packed with the core. All the chains C have the first fragment in a *gauche* conformation with an O–C–C–C torsion angle close to $\pm 60°$, while the remaining alkyl parts are quite linear

Table 4. Significant dihedral angles (°) between the aromatic rings and chains C and C′ (as labelled in figure 2) in the molecules of 7DIAB and 8DIAB.

	7DIAB		8DIAB	
Dihedral angle (°)	Molecule **1**	Molecule **2**	Molecule **1**	Molecule **2**
ϕ_2/ϕ_1	73	67	74	65
ϕ_3/ϕ_2	44	45	47	43
ϕ_4/ϕ_3	88	79	85	76
chain C/ϕ_4	88	73	77	86
chain C′/ϕ_3	11	13	3	3

and roughly planar, as frequently observed in related mesogenic structures [13]. The dihedral angles between the mean plane of alkyl chain C and the adjacent planar *p*-chlorobenzoyl part of the core (chain C/ϕ_4) are given in table 4. In the four conformers this angle is about 90°. However, the mean plane of chain C is close to that of the ϕ_3 phenyl group.

On the contrary, in all conformers, the second alkoxy lateral chain C′ (figure 2) points far away from the core. This chain is however not fully extended and consequently not planar. The mean angle between the core axis and this latter chain is about 70°. In both 7DIAB and 8DIAB, the second lateral alkoxy chain is characterized by very high thermal motion B_{eq} factors which increase from the beginning to the end of the alkyl chain; this reflects a considerable disorder. In 5DIAB and 6DIAB, the first carbons in both chains are above and below the mean aromatic plane ϕ_3, allowing the folding of the two chains along the core. It is interesting to note that in 7DIAB and 8DIAB, these two carbons are on the *same* side of the mean plane of ring ϕ_3, making it impossible for chain C′ to fold back along the core. The molecular conformation of all conformers is entirely defined by the torsion angles given in table 5.

The molecular conformations can also be described by the relative orientations of the mean core plane and the two chains, as presented in table 6. This illustrates very well the great similarity of the four conformers.

The unit cell parameters (see table 1) for the crystals of both 7DIAB and 8DIAB are very similar. Thus, it is not surprising that the conformers **1** on the one side and conformers **2** on the other (figure 2) are quite similar in the 7DIAB and 8DIAB crystal structures. The salient feature is the similarity in the geometry of conformers **1**

Table 5. Significant torsion angles (°) in 7DIAB and 8DIAB, molecules **1** and **2**: the C7–O8–N10–N11 torsion angle, when considering molecule **2**, refers in fact to the C107–C108–N110–N111 torsion angle.

		7DIAB		8DIAB	
Molecule part	Torsion angle	Molecule **1**	Molecule **2**	Molecule **1**	Molecule **2**
	C7–O8–C10–C11	118	− 113	66	− 69
	C12–C13–N16–N17	17	− 15	− 21	15
Core	N16–N17–C20–C21	25	− 29	− 27	26
	C22–C23–O26–C27	− 99	− 94	101	99
	C23–C24–O36–C37	− 109	− 108	111	109
	C24–O36–C37–C38	*trans*	165	*trans*	− 166
	O36–C37–C38–C39	− 56	− 60	53	62
Chain C	C37–C38–C39–C40	*trans*	*trans*	*trans*	*trans*
	C38–C39–C40–C41	*trans*	*trans*	*trans*	*trans*
	C39–C40–C41–C42	*trans*	*trans*	*trans*	*trans*
	C40–C41–C42–C43	157	*trans*	− 167	*trans*
	C41–C42–C43–C44	—	—	− 119	− 158
	C20–C25–O45–C46	62	60	− 61	− 65
	C25–O45–C46–C47	*trans*	*trans*	*trans*	164
	O45–C46–C47–C48	109	164	− 80	49
Chain C′	C46–C47–C48–C49	132	− 78	− 140	165
	C47–C48–C49–C50	*trans*	− 158	− 61	*trans*
	C48–C49–C50–C51	138	− 148	*trans*	*trans*
	C49–C50–C51–C52	*trans*	*trans*	147	− 145
	C50–C51–C52–C53	—	—	− 142	137

Table 6. Mean plane angles (°) giving the relative orientations of the core and the chains C and C′ in 7DIAB and 8DIAB, molecules **1** and **2**.

	7DIAB		8DIAB	
Relative orientation	Molecule **1**	Molecule **2**	Molecule **1**	Molecule *2*
Core/chain C	12	15	21	22
Core/chain C′	100	106	115	106
Chain C/chain C′	87	97	100	92

and conformers **2** in both crystal structures. According to Weissflog and Demus [1–3] the heptyl lateral chains in a series of 1,4-di-(4-*n*-octyloxybenzoyloxy)-2-*n*-alkylbenzenes were assumed to be folded and aligned along the polyaromatic central core in the nematic phase. In a more recent paper, a 2D ^{13}C NMR study of the nematic phase of 7DIAB shows that both chains are folded back along the polyaromatic central core and oriented in opposite directions [14]. This is observed in the 5DIAB and 6DIAB structures where both alkoxy chains are folded back to the polyaromatic core. This relates to the smaller bulkiness of the whole molecule which keeps the molecular anisotropy compatible with the existence of a nematic phase. More surprising are the conformations of molecules **1** and **2** for 7DIAB and 8DIAB, where one of the alkoxy chains is folded back to the polyaromatic core, while the other points far away from the core. Even with these unfavourable geometries, such molecules give a nematic phase, providing some clue about the conformation change at the solid–nematic transition.

Whilst the molecular arrangement in the 5DIAB and 6DIAB structures [5] is a typical nematic one, with the molecules strictly parallel to the same direction through the centres of symmetry of the $P\bar{1}$ space group, this is not the case in the 7DIAB and 8DIAB structures ($P2_1/a$ and $P2_1/c$ space groups, respectively). If the independent molecules **1** and **2** are quasi-parallel (their core axes make angles close to only 5° and 9°) the equivalent molecules related by the 2_1 axis and the *a* or *c* glide plane are not perfectly parallel to them. This is a common feature in nematogenic crystal structures [15, 16]. The projections of the cell for 7DIAB and 8DIAB crystal structures, respectively, on the (yOz) and (xOy) principal planes are shown in figure 3. In both structures the cohesion in the crystal is assumed to arise partly through dipole–dipole interactions between the COO polar groups [17] and partly through numerous weak van der Waals interactions. These assumptions are in agreement with the large disorder of the alkoxy chains and correspond to a rather low density close to 1.16 g cm^{-3} (compared with the average density of 1.23 g cm^{-3} obtained for the 5DIAB and 6DIAB compounds).

3.2. ^{13}C *NMR spectra in the solid and nematic phases*

Recently, we have shown for compounds having a single lateral chain that it is possible to probe the lateral chain conformation by ^{13}C NMR using the $-OCH_2-$ resonance in the solid and nematic phases [7, 8, 18]. In the case of dilaterally substituted compounds having short chains (5DIAB and 6DIAB), it was shown, that the related line position is dependent on the conformation of the lateral chain and on the interaction of the nearby lone pair oxygen leading to a difficult analysis of this line position in the solid spectrum. This problem is certainly enhanced by a longer chain, as several conformers exist in the solid phase; the assigment of the $-OCH_2-$ signals may then be difficult.

Accordingly, the ^{13}C spectra in the solid phase of the compounds studied (7DIAB, 8DIAB and 12DIAB) present many split lines with variable intensities, leading to a rather difficult interpretation. At least, we can emphasize that the existence of the different conformers affects the NMR spectrum in the aliphatic region as well as the aromatic. As an example, figure 4 presents four spectra of 12DIAB in the solid, at the T_{CrN} transition, in the nematic and in the isotropic phases. Two signals are observed for the $-OCH_2-$ carbons in the solid, nematic and isotropic phases. Amazingly, a single line is observed just at the T_{CrN} transition. In the low field part of the aromatic spectrum, two signals of nearly equal intensities are observed for each Ca and Cb carbon, clearly indicating that at least two different molecules exist in the solid phase. Thus, in the solid phase, the presence of only two lines for the $-OCH_2-$ carbons is fortitious, as four peaks should be obtained. At the transition, the upfield $-OCH_2-$ peak collapses, as well as the two inner peaks in the Ca–Cb massif, indicating that one conformer is changing structure to match the local geometry of the remaining conformer. This is a hint that in the solid phase the methyleneoxy frequencies are equal for the two carbons in each conformer. In the nematic phase and isotropic phase, a single peak is observed for the Ca and Cb carbons as expected, and two peaks are observed in the $-OCH_2-$ region. A similar complex behaviour is obtained for 7DIAB and 8DIAB. Three lines are observed is the $-OCH_2-$ region, but the line intensities

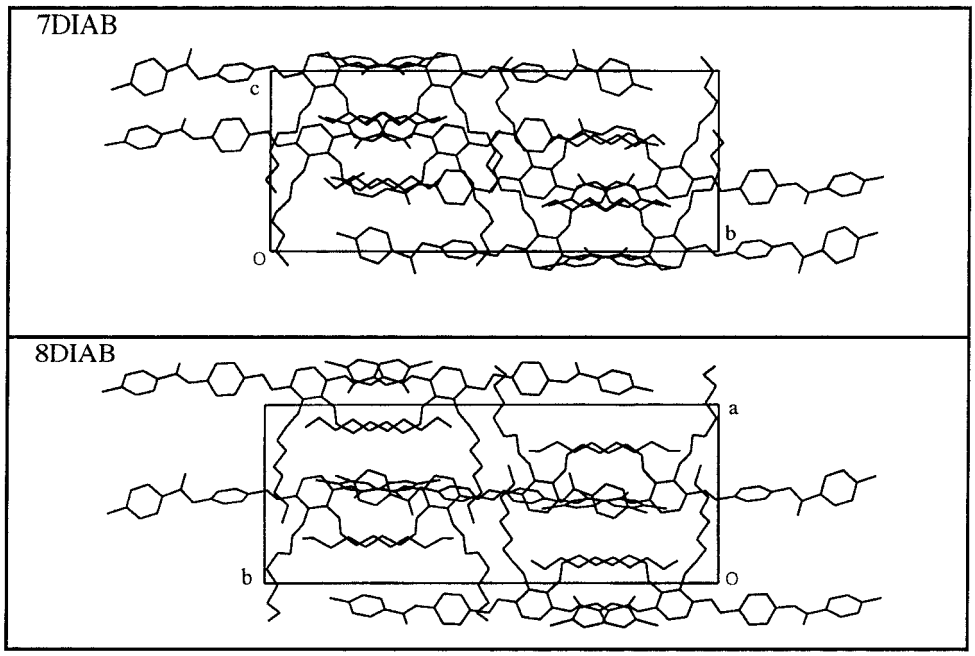

Figure 3. Projection of the 7DIAB and 8DIAB crystal structures, respectively, on the ($y0z$) and ($x0y$) planes.

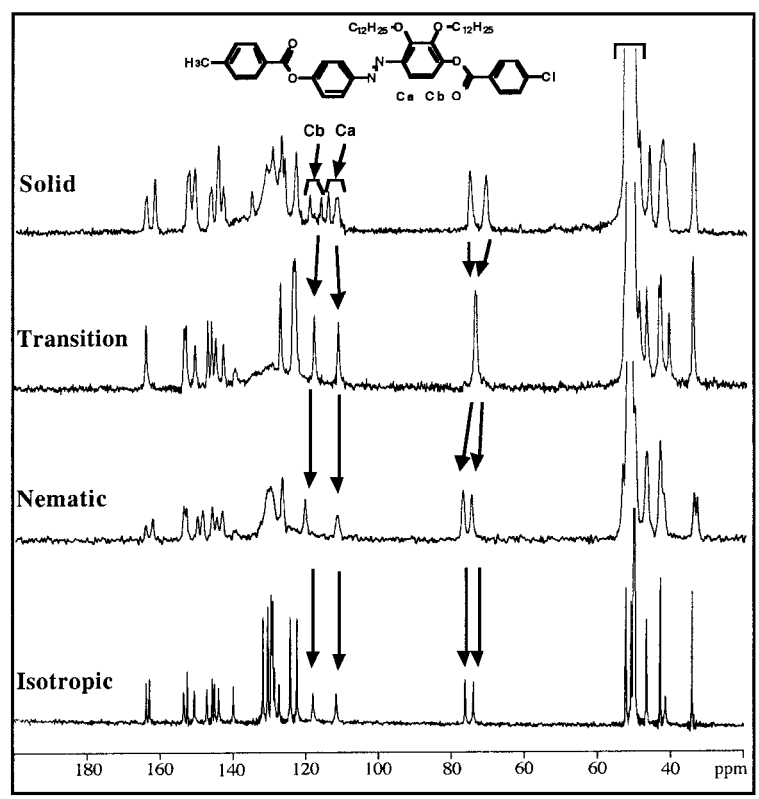

Figure 4. ^{13}C NMR spectra of 12DIAB in the solid phase 5°C below the transition Cr–N, at the transition, in the nematic phase 5°C above the transition Cr–N and in the isotropic phase.

are rather different, meaning that the relaxation times associated with each conformer are different. On further heating, the spectra are nearly equivalent even if the lines are broader, indicating that the solid obtained on cooling is essentially the same as the polycrystalline sample. This behaviour is confirmed by the equivalent DSC thermograms obtained on temperature cycling.

Figure 5 gives the chemical shift dependence of the lateral $-OCH_2-$ carbons in 7DIAB, 8DIAB and 12DIAB on increasing the temperature. In the solid phase of

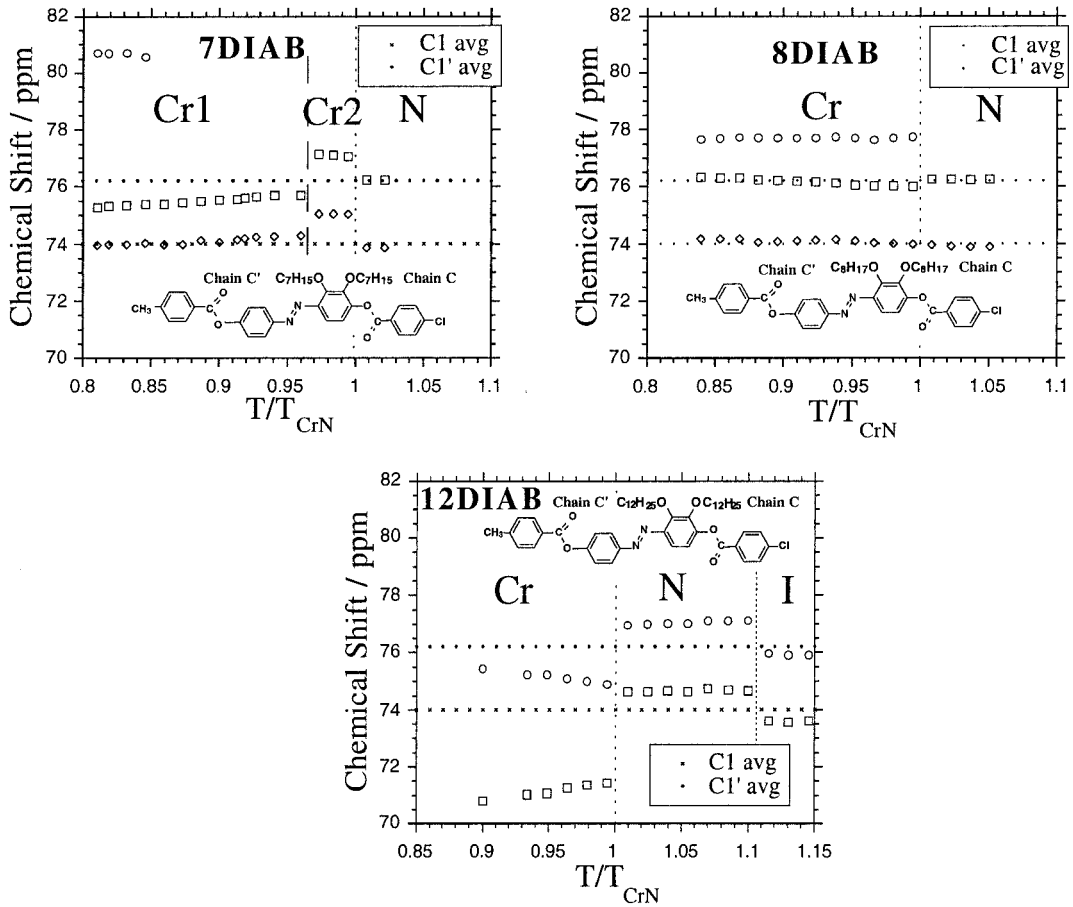

Figure 5. Chemical shift dependence of the lateral $-OCH_2-$ carbons in 7DIAB, 8DIAB and 12DIAB on increasing the temperature. $C1_{avg}$ and $C1'_{avg}$ are the average of the chemical shifts observed for the methyleneoxy carbons having chain length less than 9 carbons.

7DIAB and 8DIAB, three peaks are present in the 70–82 ppm region, the downfield peak having a smaller intensity than the other two. During the heating process, this peak disappears in the solid phase of 7DIAB. After the solid–nematic transition, two peaks remain, located at the same averaged chemical shift: i.e. 74.0 ± 0.1, 76.2 ± 0.1 ppm which can be assigned to C1 and C1′ carbons, respectively. In the nematic phase of 12DIAB, the observed chemical shifts are above the averaged values observed for compounds with smaller chains. In fact, if we assume the folding of the chain, the chain C′ overlaps the core up to 8 carbons in the chain. Thus, in 12DIAB the far part of the chain does not overlap the core and this can modify the geometry around the methyleneoxy carbons.

4. Conclusion

The X-ray structures of two compounds (7DIAB and 8DIAB) containing four rings in the main core and two lateral chains have been solved. Their space groups are $P2_1/a$ or $P2_1/c$, respectively with two independent molecules in the cell. If these two molecules are quasi-parallel, the equivalent molecules which are related by the 2_1 axis and the a or c glide plane are not perfectly parallel to them. In both structures, the common four-ring central core is extended and quite rigid, with a total length close to 28.5 Å. One alkoxy lateral chain is folded back along the core and the second points far away from the core. These molecular arrangements, are generally not good in a precursor for the appearance of the liquid crystal phase. The ^{13}C MAS NMR spectra of the three compounds were obtained upon temperature increase. The existence of several conformers is clearly seen in the aliphatic, as well as in the aromatic region, for all compounds. After the solid–nematic transition, the frequencies of the first two lateral carbons are nearly identical whatever the dialkylated compound involved, showing that the mean conformation in the nematic phase of the first fragment is fairly independent of the chain length. This shows the conformational change of the chain that occurs when entering the nematic phase.

References

[1] Weissflog, W., and Demus, D., 1983, *Cryst. Res. Tech.*, **18,** K21.
[2] Weissflog, W., and Demus, D., 1984, *Cryst. Res. Tech.*, **19,** 55.
[3] Weissflog, W., and Demus, D., 1985, *Mol. Cryst. liq. Cryst.*, **129,** 235.
[4] Demus, D., 1989, *Liq. Cryst.*, **5,** 75.
[5] Allouchi, H., Belaaraj, A., Cotrait, M., Lafontaine, E., Judeinstein, P., and Bayle, J-P., 2000, *Liq. Cryst.*, **27,** 1087.
[6] Perez, F., Berdaguè, P., Judeinstein, P., Bayle, J-P., Allouchi, H., Chasseau, D., Cotrait, M., and Lafontaine, E., 1995, *Liq. Cryst.*, **19,** 1015.
[7] Perez, F., Berdaguè, P., Judeinstein, P., Bayle, J-P., Allouchi, H., Cotrait, M., and Lafontaine, E., 1996, *Liq. Cryst.*, **21,** 855.
[8] North, A. C. T., Phillips, D. C., and Mathews, F. S., 1968, *Acta Cryst.*, **A24,** 351.
[9] Gilmore, C. J., 1984, *J. appl. Crystalogr.*, **17,** 42.
[10] Sheldrick, G. M., 1993, Program for the Refinement of Crystal Structures, University of Göttingen, Germany.
[11] Haw, J. F., 1988, *Anal. Chem.*, **559A,** 60.
[12] Kromm, Ph., 1995, PhD thesis, University of Bordeaux, France.
[13] Allouchi, H., 1994, PhD thesis, University of Bordeaux, France.
[14] Perez, F., Bayle, J.-P., Fung, B. M., 1996, *New. J. Chem.*, **20,** 537.
[15] Sato, T., and Yano, S., 1987, *Mol. Cryst. liq. Cryst.*, **144,** 179.
[16] Walz, L., Haase, W., and Eidenschink, R., 1989, *Mol. Cryst. liq. Cryst.*, **168,** 169.
[17] Zareba, I., 1997, PhD thesis, University of Bordeaux, France.
[18] Perez, F., Berdaguè, P., Judeinstein, P., Bayle, J.-P., Allouchi, H., Chasseau, D., Cotrait, M., and Lafontaine, E., 1995, *Liq. Cryst.*, **19,** 345.